

# Photon-Pair Generation in a CMOS Microring: Impact of Spontaneous Raman Scattering and Its Mitigation

Anirudh Ramesh<sup>1†</sup>, Imbert Wang<sup>2</sup>, Đorđe Gluhović<sup>2</sup>, Danielius Kramnik<sup>3</sup>, Josep M. Fargas Cabanillas<sup>2</sup>, Kim F. Lee<sup>1</sup>, Vladimir Stojanović<sup>3</sup>, Miloš A. Popović<sup>2</sup>, and Prem Kumar<sup>1‡</sup>

<sup>1</sup>Center for Photonic Communication and Computing, Dept. of Electrical and Computer Eng., Northwestern University, Evanston, IL 60208, USA

<sup>2</sup>Department of Electrical and Computer Engineering, Boston University, Boston, Massachusetts 02215, USA

<sup>3</sup>Department of Electrical Engineering and Computer Science, UC Berkeley, Berkeley, CA 94720, USA

<sup>†</sup>anirudh@u.northwestern.edu, <sup>‡</sup>kumarp@northwestern.edu

**Abstract:** We study spontaneous four-wave mixing and spontaneous Raman scattering (SpRS) in a CMOS microring cavity in the C-band and find that the latter contributes a significant fraction to the signal/idler photon flux. We expect operation in the O-band to be less affected by SpRS due to higher confinement of the O-band light in crystalline Si in this device. © 2022 The Author(s)

Silicon photonics is a promising platform for pair sources with photon-pairs generated by spontaneous four-wave mixing (SFWM) as a result of the third-order ( $\chi^{(3)}$ ) optical nonlinearity of crystalline silicon (c-Si) [1]. In addition, the Si CMOS platform used to manufacture electronics has been successfully adapted to fabricate chip-based photonics with zero change [2], having the advantage of monolithic integration of electronic circuits alongside photonic circuits. We previously demonstrated a microring resonator based on-chip source in CMOS with integrated tunable pump filtering and closed-loop feedback stabilization of SFWM [3,4], shown in Fig. 1(a),(b). The performance metrics of these devices are affected by generation of noise photons, a significant source being spontaneous Raman scattering (SpRS), a  $\chi^{(3)}$  effect as well. This device generates photon-pairs by SFWM at a detuning of  $\approx 1$  THz from the pump. c-Si has a relatively narrow ( $\approx 100$  GHz wide) Raman response at a 15.6 THz detuning, thus we can ignore the SpRS contribution from the core. The fixed thickness of the c-Si layer ( $<100$  nm) of the CMOS (in this case, the GlobalFoundries 45RFSOI) fabrication process of these devices causes the waveguide mode to extend out of the c-Si core and into the cladding comprised of amorphous silicon dioxide and silicon nitride, both of which have a broadband Raman response. This causes the generation of SpRS photons along with the quantum-correlated photon pairs in the signal and idler channels of the device. In order to characterize the extent of SpRS in the devices operating in the C-band, we study the single photon counts in both the signal and idler channels by pumping the microring at resonance. The following equation:  $n_u = \Delta v_u \int (|\gamma P_0 L|^2 + P_0 L |g_R| N_u) dt$  [5] predicts the number of photons generated in the signal/idler channel in a regime where SFWM and SpRS are the dominant nonlinear effects, which is dictated by the pump intensity on-chip [2]. Here,  $u$  is the channel,  $P_0$  refers to the instantaneous pump power,  $\Delta v_u$  refers to the filter bandwidth,  $\gamma$  refers to the Kerr nonlinear coefficient,  $g_R$  is the Raman gain,  $L$  is the interaction length, and  $N_u$  is the phonon population. We fit the singles counts to a second order polynomial in  $P_0$ , and constrain the coefficients to be positive. The number of photons generated by SpRS varies linearly with pump power whereas the number of

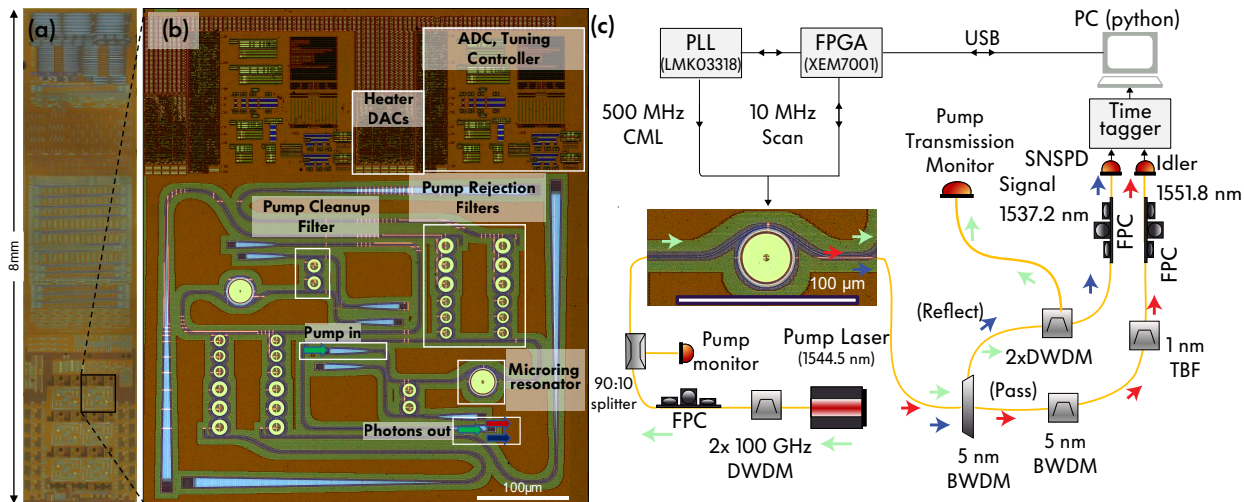


Fig. 1: (a) Electronic-photonic quantum system-on-chip (EPQSoC) with (b) two system sites with circuits on chip. We measure solely the microring resonator as indicated. (c) Experimental setup for measuring singles photon counts.

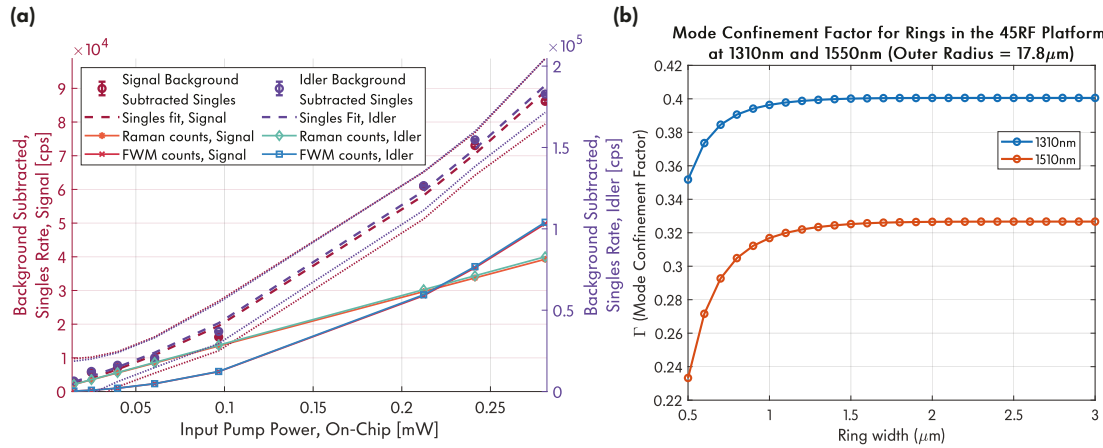


Fig. 2: (a) Singles counting results for this device along with the fit, from which the SpRS and SFWM photons counts are estimated as a function of pump power ( $\lambda_p = 1544.5$  nm). The dotted lines show the 95% confidence interval for the fit. The error bars for the data are within the markers, and calculated as the square root of the singles counts, which are assumed to be Poisson distributed. (b) Mode simulated for the C-band and the O-band microrings with varying widths.

SFWM photons varies quadratically [6], thus allowing us to estimate the proportion of SpRS and SFWM counts in each channel by extracting those terms from the fit. Before fitting, we also subtract the singles counts obtained by pumping the system off-resonance to only obtain counts generated in the microring due to resonant field enhancement. We use the linear least squares method to fit our data and achieve a R-squared value of 0.9969 and 0.9952 for the idler and signal data respectively.

Fig. 1(b) shows the experimental setup for the quantum characterization of the microrings. In our previous work [6], we did not properly account for the effect of the variation in the field enhancement near resonance for individual data points. This affected both the SpRS and SFWM processes inconsistently, as a result of which we calculated a negligible contribution of SpRS to our singles counts. In this work, we correct this by monitoring the optical transmission of the pump as well, which indicates the extent of alignment of our pump with the cavity resonance wavelength, thus ensuring that all our measurements have the same field enhancement. We achieve this by using the on-chip electronics to thermally tune [3] the cavity response as needed for consistent field enhancement for all our measurements. Our analysis indicates a significant contribution from SpRS to the singles photon counts as shown in Fig. 2(a).

We define the mode confinement factor ( $\Gamma$ ) to be the ratio of the propagating component of the Poynting vector within the c-Si core region to that in the entire waveguide cross-section. Simulating the  $\Gamma$  for a range of waveguide widths, as shown in Fig. 2(b) for a microring of radius 17.8  $\mu\text{m}$  using a finite-difference numerical modesolver, we find that a mode propagating in the waveguide in the O-band would be more confined to the core as compared to the C-band, also leading to less of the mode being in the cladding where SpRS occurs. Since both  $g_R$  and  $\gamma$  are expected to scale similarly with wavelength, we can expect lesser SpRS in this device while operating in the O-band versus the C-band for the same pair-generation rate. Quantum communications in the O-band is a rapidly developing field which also involves coexistence of O-band quantum signals with classical signals in the C-band in the same channel [8]. Thus O-band CMOS-based pair sources could be a potential candidate for applications in quantum networking.

**Acknowledgments:** Work funded in part by NSF EQuIP grant 1842692, the Catalyst Foundation, and the ONR grant N000141410259. We thank Ayar Labs and GlobalFoundries for support in fabrication.

## References

1. J. Sharping *et al.*, "Generation of correlated photons in nanoscale silicon waveguides ...", Optics Express, 14, 12388-12393 (2006).
2. C. Gentry, *et al.* "Quantum-correlated photon pairs generated in a commercial 45 nm complementary... ", Optica, 2, 1065-1071 (2015).
3. I. Wang, J.M. Fargas Cabanillas, D. Kramnik, A. Ramesh, *et al.*, "Toward quantum electronic-photonic ...", SM3N.2, CLEO (2022).
4. J. Fargas-Cabanillas, D. Kramnik, A. Ramesh, *et al.*, "Tunable Source of Quantum-Correlated Photons...", FTu2E.1, FiO (2021).
5. Q. Lin and Govind P. Agrawal, "Silicon waveguides for creating quantum-correlated photon pairs," Opt. Lett. 31, 3140-3142 (2006).
6. A. Ramesh *et al.* "Photon-Pair Generation in a 45 nm CMOS Microring Cavity: Impact of Spontaneous ...", QTh2B.4, Quantum 2.0, (2022).
7. M. A. Popović, "Complex-frequency leaky mode computations using PML...", In Integrated Photonics Research, ITuD4, (2003).
8. J.M. Thomas *et al.* "Entanglement Distribution in Installed Fiber with Coexisting Classical ....", Tu3I.3, OFC, (2022).